

GEOSTATISTICAL INVERSION OF GRAVITY AND WELL-LOG DATA

ROSA JIMÉNEZ¹ & MIGUEL BOSCH²

¹ Laboratory of Geophysical Simulation and Inversion, Department of Applied Physics, Universidad Central de Venezuela, Caracas. Presently at San Diego State University, California.

² Laboratory of Geophysical Simulation and Inversion, Department of Applied Physics, Universidad Central de Venezuela, Caracas. e-mail: miguel.bosch@ucv.ve; rjimenez@sciences.sdsu.edu

Recibido: noviembre de 2007

Recibido en forma final revisado: mayo de 2008

RESUMEN

We developed and applied a gravimetric inversion methodology that combines well-log and gravity information in a geostatistical framework. This technique looks for the optimal model that explains the geophysical data and satisfies the prior information on the model parameters, by solving iteratively a system of linear equations to update the 3-dimensional mass density field and the interface geometry between model layers. The optimal model jointly explains the gravity observations, complies with the prior statistical distribution of the mass density and honors well constraints on the interface between layers. We apply the technique to a set of data in eastern Venezuela to analyze the prediction errors on the sedimentary basin basement depth, and particularly the effect of progressively including more well constraints into the geostatistical inversion. The inversion process combining gravity and well data always produced a better prediction of the basement depth than the gravity inversion with no well control on the basement. We compared the basement depth estimates of the geostatistical inversion with the results obtained from plain interpolation of the well data (*e.g.* Kriging) and found that the geostatistical inversion of gravity data with well constraints improved the basement estimation when the spatial distribution of the wells is scarce, and both methods are equivalent when the spatial distribution of the wells is dense.

Keywords: Inversion, Gravity data, Orinoco belt, Well-long data, Geostatistics.

INVERSIÓN GEOESTADÍSTICA DE DATOS DE GRAVEDAD Y REGISTROS DE POZO

ABSTRACT

En este trabajo se desarrolló y aplicó una metodología de inversión que combinó datos de registros de pozo y de gravedad bajo una formulación geoestadística. En esta técnica se realizó una búsqueda de la configuración óptima del modelo que explica los datos geofísicos y satisface la información previa sobre los parámetros del modelo, mediante la solución iterativa de un sistema lineal de ecuaciones para actualizar el modelo tridimensional de densidades de masa y la geometría de las superficies entre las capas del modelo. La configuración óptima explica las observaciones de gravedad, es consistente con la información estadística previa y ajusta a los datos de pozos sobre la localización de las capas del modelo y los valores de densidad. Aplicando la técnica a un conjunto de datos en la región oriental de Venezuela para analizar los errores de predicción de la profundidad del basamento cristalino y el efecto de incluir progresivamente más información de pozos como restricción en la inversión geoestadística. El proceso de inversión que combina datos de gravedad y de pozos produce una mejor predicción de la profundidad del basamento que la inversión de gravedad sin control de pozos. Se comparó la estimación de la profundidad del basamento obtenida con la inversión geoestadística con los resultados obtenidos de la interpolación geoestadística simple de los datos de pozos (método de Kriging) y se encontró que la inversión geoestadística de datos de gravedad, condicionada por la información de pozos, mejora los estimados de la

profundidad del basamento cuando la distribución espacial de los pozos es escasa, y ambos métodos proporcionan resultados similares cuando la distribución espacial de los pozos es densa.

Palabras clave: Inversión, Gravimetría, Faja del Orinoco, Datos de pozo, Geoestadística.

INTRODUCTION

The certainty on the results of the gravity data inversion is commonly affected by the non-uniqueness of the solution, data errors and the variability of the mass density within the geological bodies considered in the model. Due to this characteristic, it is useful to consider an inversion scheme that takes into account other types of information in addition to the gravity data, to better constraint the results to realistic model configurations. New inversion methodologies based on a probabilistic approach (Tarantola, 1987; Mosegaard & Tarantola, 2000; Bosch, 1999) allow to combine *a priori* geological, petrophysical and geostatistical information with the geophysical observations. The formulation based on this approach has been solved with different techniques, such as Monte Carlo sampling (Bosch *et al.*, 2001; Bosch & McGaughey, 2001) and optimization (Jiménez *et al.*, 2002; Jiménez & Bosch, 2004; Jiménez, 2004; Bosch *et al.* 2006).

We formulate an inversion method that combines the gravity data with well-log information about the geological interfaces depths and density statistics within model layers, and apply this method to estimate the top of the basement in a sedimentary basin located in eastern Venezuela, South America. With this method, we jointly estimate the geometry of model interface between layers and the 3-dimensional density field within each layer, the latter honoring prior spatial statistics.

The estimation of the depth of the interface between model layers and the estimation of the density field with the inversion of gravimetric data have been aspects commonly studied separately. For example, in the work by Bear *et al.* (1995) and Li *et al.* (1998) a 3-dimensional density model was estimated from the observed gravity field. On the other hand, the work by Rama *et al.* (1999) and Barbosa *et al.* (1997a and 1999b) have focused on estimating the depths of the interface between two homogeneous media. Other authors as Bhaskara *et al.* (1991) considered the variability of the density as a function of the depth for the estimation of the interface depth, and Graterol *et al.* (1998) described how to produce a basement map using a variable datum and seismic information. The work by Gallardo-Delgado *et al.* (2003) jointly estimates the interface depths and the density contrast, the latter modeled as a polynomial function dependent with depth, inverting gravity and magnetic data.

In this work we describe a methodology developed by

Jiménez *et al.* (2002); Jiménez (2004) for 3D geostatistical inversion of gravimetric data, based on an iterative optimization of the model configuration to jointly fit the gravity observations and the geostatistical model for layer densities and interfaces. In this way the solution explains the gravity data and also satisfies well constraints and density spatial statistics. We apply this methodology to an area of the Orinoco Belt, Venezuela, evaluate the effect of combining gravity data and well data for the basin basement estimation, and show the results of the progressive increase of the number of well constraints into the inversion.

METHODOLOGY

A first step in our method is to describe, in three-dimensions, the mass density field within two different lithological layers and the geometry of the interface between them. We divide the volume within each layer in rectangular prisms, or *blocks*, of homogeneous mass density, and the interface that separates the layers in corresponding rectangular pieces as shown in Figure 1. The blocks are not regular as they conform to the arbitrary position of the interface between the layers. Our model parameters are the mass density in each one of the prisms and the depth of each rectangular piece of the interface. We calculate the gravitational vertical acceleration due to each block separately, and then these contributions are added to obtain the calculated gravity field of the model.

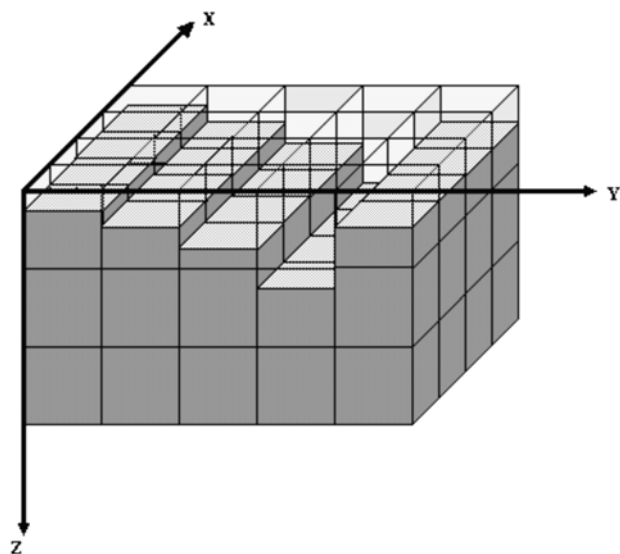


Figure 1. Volume parameterized in rectangular prisms and the surface between the upper and lower layers parameterized in rectangular pieces.

Following the approach of previous work (Bosch, 1999; Jiménez *et al.* 2002) the different types of information (geophysical, geological and petrophysical) are modeled by *probability density functions (pdf)*, which are defined either in the data space or in the model parameter space. The result of the combination of these types of information is summarized in the *a posteriori pdf* $\sigma(m)$, calculated with the product (Tarantola, 1987):

$$\sigma(m) = c L(m) \tilde{n}(m), \quad (1)$$

where m is the array of model parameters that describes both the mass density field and basement depths, $\tilde{n}(m)$ is the prior *pdf* that describes the prior information on the model parameters, $L(m)$ is the likelihood function that measures the fit between the observed and calculated data, and c is a normalization constant.

We model the *a priori* information on the model parameters with a multivariate Gaussian function, $\tilde{n}(m) = c \exp[-\frac{1}{2}(m - m_{\text{prior}})^t C_M^{-1}(m - m_{\text{prior}})]$, where m_{prior} is the mean of the *a priori* statistical model and C_M is the prior model covariance matrix. The upper-script t indicates array transposition. The covariance matrix contains in the diagonal the prior variances of the density and the depth of the interface. Prior covariances are present in the non-diagonal elements of the matrix, describing the spatial correlation of the density as a three-dimensional field and the spatial correlation of the interface depths as a two-dimensional field. We assume the spatial homogeneity of the covariance within each layer to calculate the terms of the matrix from a covariance function that depends on the distance and directions between cells, as commonly done in geostatistical work (*e.g.* Isaaks and Srivastava, 1989).

We model the likelihood function assuming Gaussian data errors, $L(m) = c \exp[-\frac{1}{2}(d^{\text{calc}} - d^{\text{obs}})^t C_D^{-1}(d^{\text{calc}} - d^{\text{obs}})]$, where d^{calc} is the gravity data calculated from the model, d^{obs} is the observed data, and C_D is the data covariance matrix. We assumed independence of data errors and hence used a diagonal data covariance matrix. The likelihood function is based in deviations between observed and calculated data, the latter obtained from the model parameters after solving the forward problem, $d^{\text{calc}} = g(m)$, which is not linear because the data depend on the interface depth in a non linear way. Thus, from equation (1) and the correspondent expressions for the likelihood function and the prior *pdf*, our posterior *pdf* is given by:

$$\sigma(m) = c \exp[-\frac{1}{2}(d^{\text{calc}} - d^{\text{obs}})^t C_D^{-1}(d^{\text{calc}} - d^{\text{obs}}) - \frac{1}{2}(m^n - m_{\text{prior}})^t C_M^{-1}(m^n - m_{\text{prior}})]. \quad (2)$$

The problem of finding the model configuration corresponding to the maximum of the posterior density is equivalent to the problem of finding the minimum of the «objective» function:

$$S(m) = (d^{\text{obs}} - d^{\text{calc}})^t C_D^{-1}(d^{\text{obs}} - d^{\text{calc}}) + (m^n - m_{\text{prior}})^t C_M^{-1}(m^n - m_{\text{prior}}), \quad (3)$$

which is the twice and opposite of the exponential argument of the posterior density. In this function, the first term measures the distance between calculated and observed data, and the second term measures the distance between the *a priori* model and the resulting model from the inversion. Minimizing the function $S(m)$ means to look for an optimal model that reduces the residual of the data and at the same time satisfies the *a priori* information. The minimum is obtained here following the Newton's method and solving iteratively the system of equations:

$$(C_M G^t C_D^{-1} G + I) \Delta m = C_M G^t C_D^{-1}(d^{\text{obs}} - d^n) - (m^n - m_{\text{prior}}) \quad (4)$$

where m^n are the current model parameters, and Δm is the solution vector that is used to update the values of the model parameters considered, $m^{n+1} = m^n + \Delta m$. The matrix G is the Jacobian matrix of the calculated gravity data function $g(m)$, containing the partial derivatives of the calculated data to the model parameters.

APPLICATION TO HAMACA REGION DATA

The Hamaca region is part of the southern flank of the Eastern Basin of Venezuela and it presents a sedimentary sequence that includes sediments from the Paleozoic to the Recent. Sediments rest on pre-cambrian rocks represented by the Igneous-Metamorphic Complex of Guayana (Feo-Codecido *et al.* 1984; Russo and Speed, 1994). Gravity data, well information on mass densities and basement depths are available on this area, which let us implement this methodology and compare results on basement estimation.

Figure 2 shows the area used for the inversion that has an extension of 120 km in X direction (EW direction) and 100 km in Y direction (NS direction), and the corresponding observed Bouguer anomaly. Notice the significant variations of the gravity field, which can be due to either heterogeneities of the density or the configuration of the sediments-basement interface. Also the anomaly shows the major structural features of the basement, indicating that it increases its depth northwards, towards the Eastern Basin depocenter. The total range of the anomaly in the area is approximately 70 mGal, and we used for the inversion a data error of standard deviation of 5% of this range (3.5 mGal) to encompass the errors associated with instrument

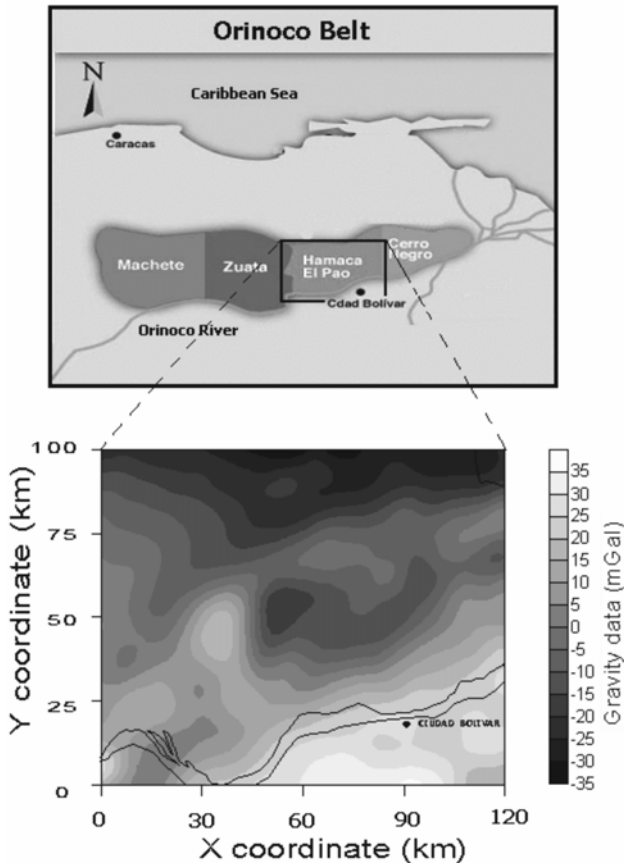


Figure 2. (top) Map of northern Venezuela showing the location of the area under study in this work, the coast line, the Orinoco river and the Orinoco oil belt area. (bottom) Bouguer gravity anomaly in the area.

measurements, calculation of the Bouguer anomaly, and simulation of the gravity data.

We consider information on values of the mass density reported in a group of 21 wells that are located in the area. Figure 3 shows their locations and the estimated basement map interpolated with a conventional Kriging method from the basement depths reported on the well locations. Figure 4 presents an example of a density-log corresponding to one of the wells and shows that the contrast of mass density between sedimentary rocks and crystalline basement is important in this area.

This information, the density data in the 21 wells used in the study, was statistically characterized to obtain the mean value and the standard deviation of the mass density for the two layers in the model. Figure 5 shows the density histograms with the mean and standard deviation values obtained for each layer, and the significant mass density contrast of approximately 600 kg/m^3 between the upper layer (sediments) and the lower one (basement) in the considered area.

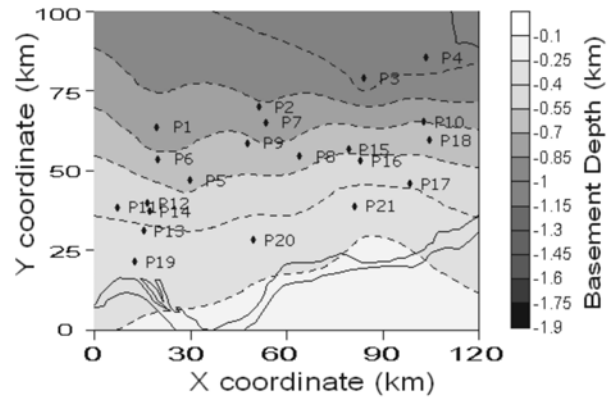


Figure 3. Map of basement depths obtained by interpolating (Kriging) depths to the basement interpreted in the 21 well-logs available in this study. Points indicate well locations.

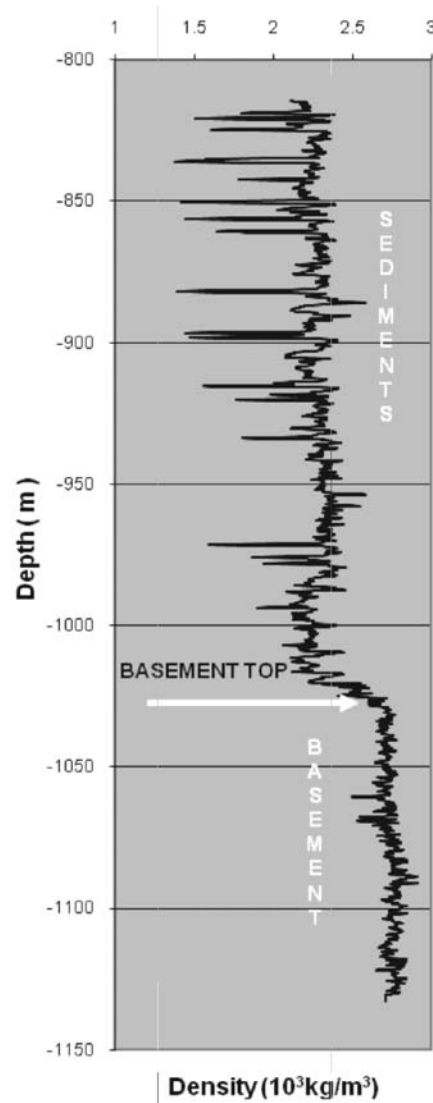


Figure 4. A representative density log of a well in the area under study, which shows the presence of two major layers (sediments and basement).

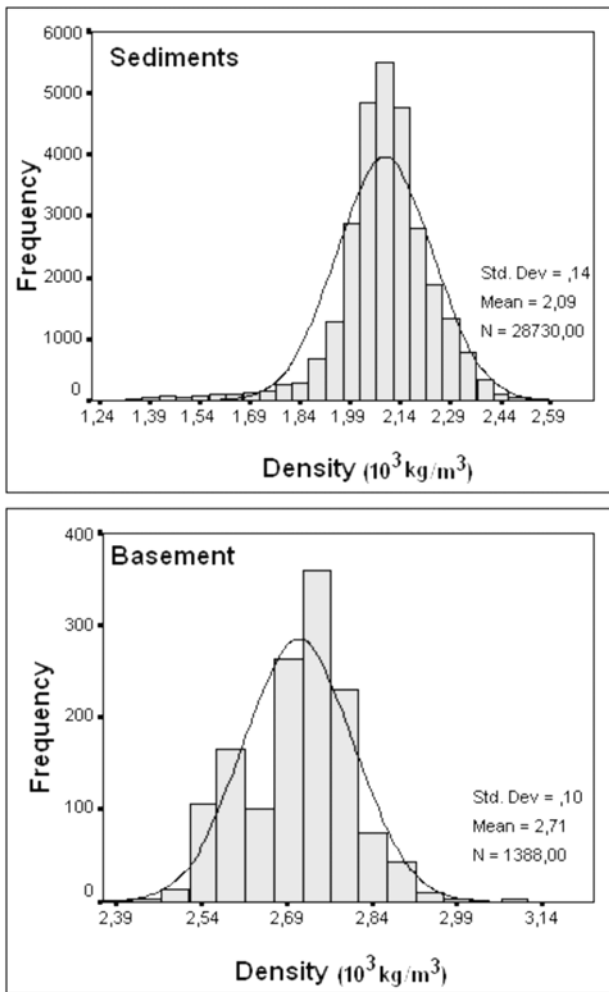


Figure 5. Histograms of the mass density corresponding to sediments and basement, obtained from the well-logs in the area.

The *a priori* model is built from two kinds of available information having effect one of them on mass density parameters and the other one on interface depth parameters. As previously mentioned, the statistical prior model is multivariate Gaussian and depends on the prior mean and covariances of the parameters that describe the information available from the well data. The prior surface corresponding to the mean basement depth is obtained making a conventional interpolation (using Kriging) of the corresponding depth reported in the wells. The prior variance associated to the surface depth is not uniform, as it is small in the interface pieces intercepting a well and larger in the interface pieces not intercepted by a well. For the latter, the depth of the basement will be controlled by a compromise between the gravity data fit and the depth on near by wells according to the covariance function used. For the inversion we used a standard deviation of the interface depth of 1 m in the interface pieces intercepted by a well and 500 m for the interface pieces not intercepted by the wells.

In the same way we prepare the prior model for the density, assigning to the cells intercepted by the wells the average well-log density in the interception, and interpolating with Kriging densities in cells that are not intercepted by the wells. We used standard deviations for the density according to the variability in the histograms for blocks not intercepted by the wells and much smaller for cells intercepted by the wells.

We did not obtain a covariance function for the density or basement depth from the well data because of the scarcity of well data in horizontal direction. We used a Gaussian covariance function model and the corresponding ranges (correlation distances) as a method to regularize in space our density fields and the basement surface. For the density field we used a covariance horizontal range (both *X* and *Y* directions) of 15 km and a vertical range of 1 km., in sediments and crystalline basement. For the basement surface we used a range of 60 km (both in *X* and *Y* directions). Also for scarcity of lateral sampling, particularly for the basement layer, we preferred to use the mass density deviation obtained at the scale of well sampling as prior standard deviation instead of reducing it by smoothing density values to the size of model blocks.

RESULTS

With this method we built six prior statistical models, differing in the quantity of wells that enter in the definition of the *a priori* model for the basement interface and the property fields. The number of wells taken into account (group A) was consecutively: 1, 3, 6, 9, 12 and 15 for a total of 6 inversion exercises. In figure 6 we show the maps of the *a priori* mean basement for each case. In each of the cases the wells not taken into account for the model (group B) were used as blind group to evaluate the basement prediction of the inversion. For the cases of 1 well and 3 wells a plane model of the interface was built, while for the remaining ones the method of Kriging was used, always satisfying the information of the wells of the group A. Additionally, we performed an inversion using no well data constraint on the basement depths.

Figure 7 shows the series of estimated basement maps obtained from the geostatistical inversion of gravity data for each of the 6 cases. It is important to remember that the technique modifies the basement depths and the density field to explain the gravimetric anomaly, at the same time it honors the depth of basement reported in the subset of wells used as *a priori* constraint and the spatial statistical model for the density field and basement surface. The maps shown in figure 7 represent the result of the estimate of the basement depth combining gravimetric information and well data, progressively increasing the content of well data information into the inversion.

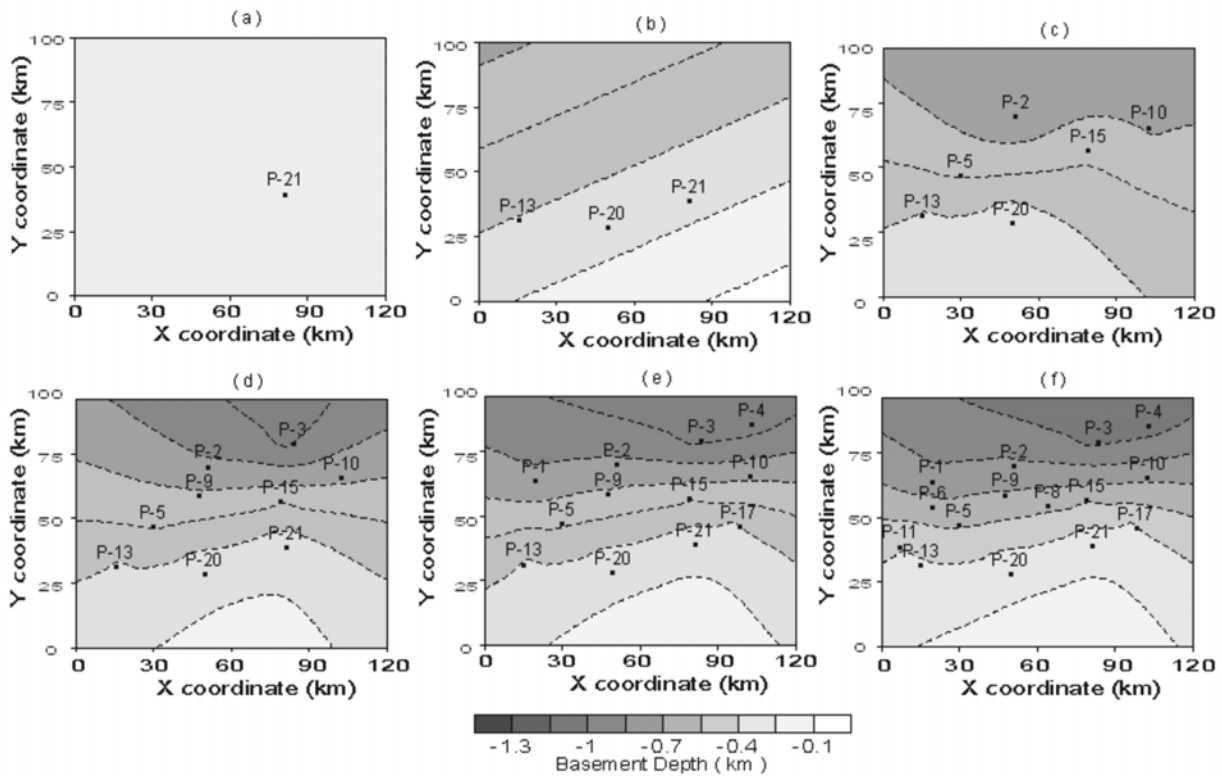


Figure 6. Maps of the *a priori* mean basement depth, built with the information of (a) 1 well, (b) 3 wells, (c) 6 wells, (d) 9 wells, (e) 12 wells, and (f) 15 wells.

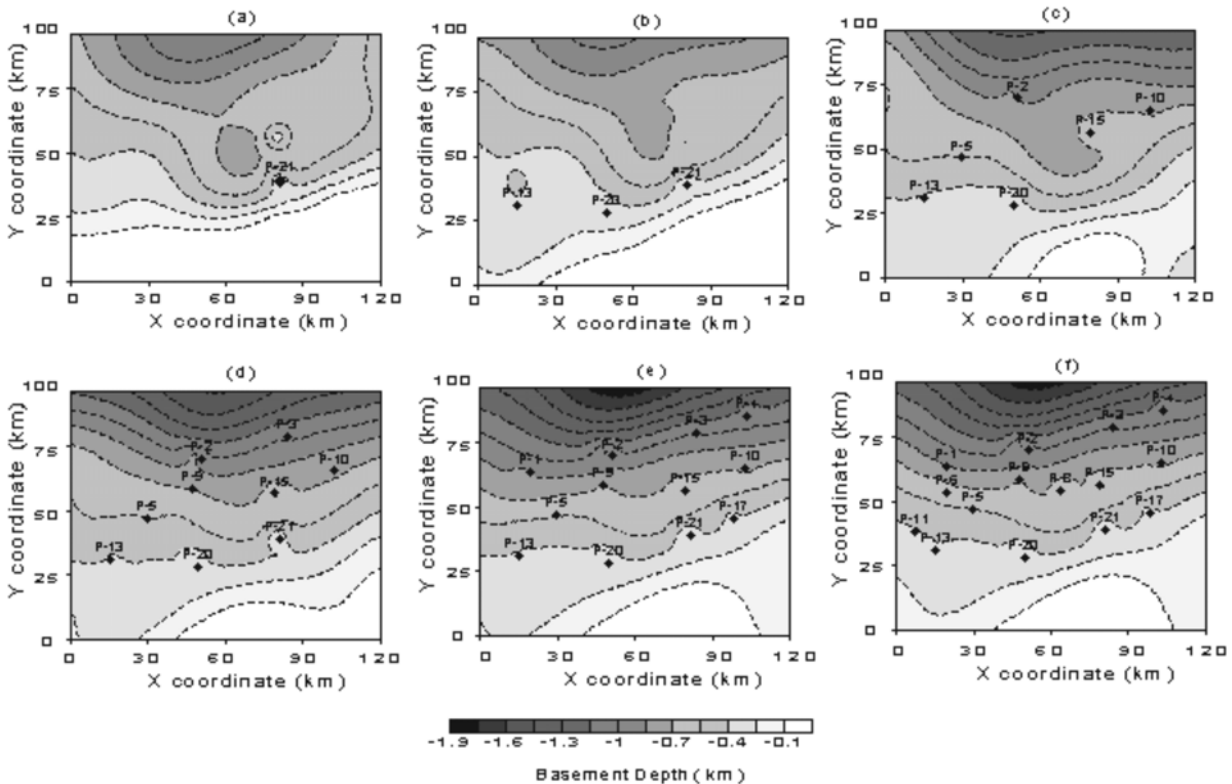


Figure 7. Basement depth maps obtained with the geostatistical inversion of gravity data from each of the prior models shown in figure 6, corresponding to constraints of (a) 1 well, (b) 3 wells, (c) 6 wells, (d) 9 wells, (e) 12 wells, (f) 15 wells.

Figure 8 shows the gravimetric fields calculated from the resulting models obtained in each of the inversion cases shown in Figure 7. The calculated gravity anomalies are similar between them and similar to the observed field (Figure 2). They reproduce also the spatial resolution of the observed field, *i.e.* the apparent wave-number composition in the data, the gravimetric anomaly extremes northward, southward at the center and even in the borders of the area. Therefore, all the models obtained in the 6 inversion cases explain the observed gravity data satisfactorily, within the data errors considered.

Models obtained with the inversion include also the three-dimensional density fields in the sediment and basement layers. Figure 9 shows two vertical sections of the density field for the solution of the inversion case corresponding to 15 wells constraining the model. The variability of the density in the inverted models complies with the prior statistics used in the inversion. Figure 10 shows the mass density histogram obtained from the estimated model in the inversion case of 15 wells (basement shown in figure 7f and calculated gravity in Figure 8f). The mean values of the density for the sediments and the basement rocks reproduce very well the mean values as obtained from the well data shown in Figure 5. Deviations are also comparable, although smaller in the

inverted model, as expected due to the change of scale between large cells used in the inversion and the well sampling scale used for the histograms of Figure 5.

Additionally, we carried out an inversion of gravity data with no well depths constraints in the basement. Statistics for the mass density fields were the same as the statistics used in the cases already shown, centered in the corresponding mean value for the density in the sediment and basement layers. The prior model for the basement depth was a flat surface in the mean value of well depths. Figure 11 shows the basement depth map estimated with the inversion, which basically reproduces all features of the observed gravity data (Figure 2) into the predicted basement structure.

This includes the positive-negative gravimetric anomaly couple at the center of the area that does not correspond to a basement feature as shown by the well data. Inversions combining well and gravity data explain this gravity observation with the lateral density changes within the crystalline basement rocks (Figure 9).

From the optimal models obtained in each inversion case (basement shown in Figure 7) we compare the basement depth prediction with the well-known value of the basement

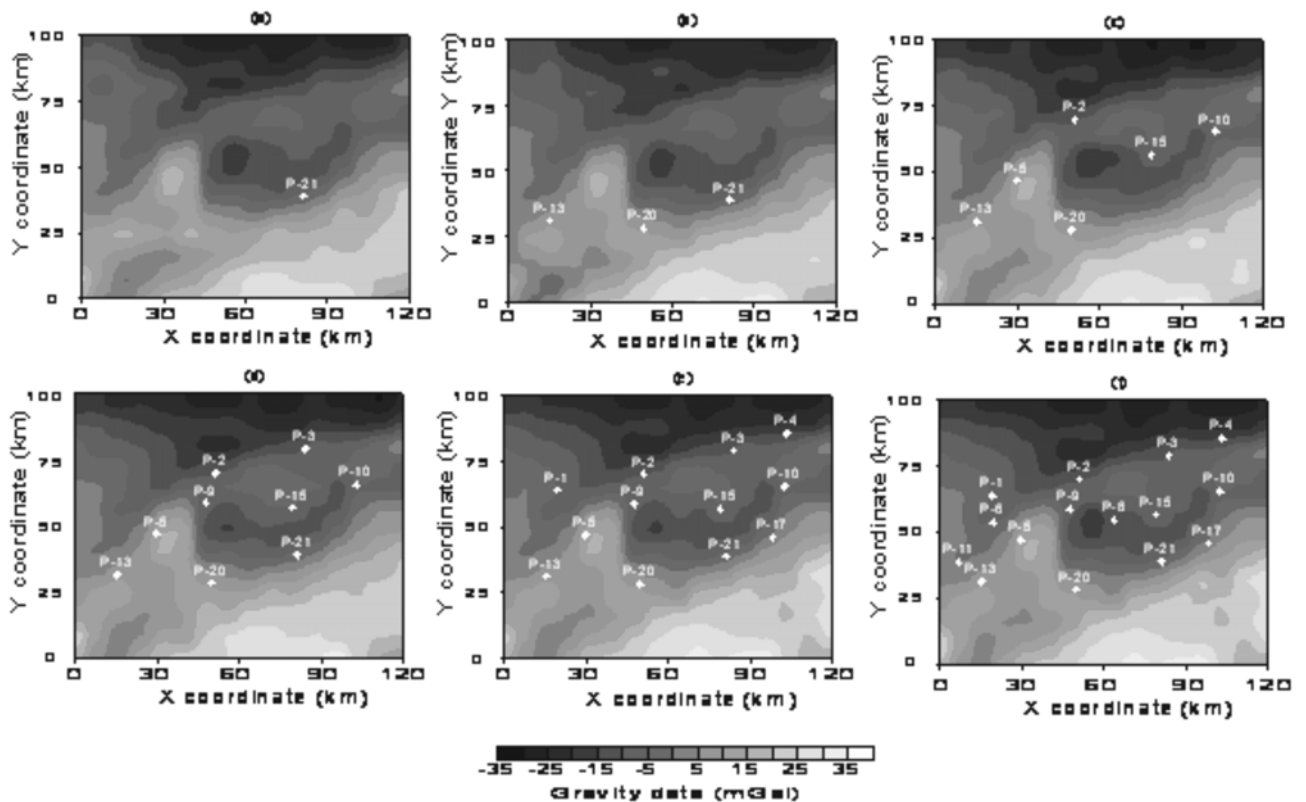


Figure 8. Gravity anomaly maps calculated from the models obtained in the geostatistical inversion, corresponding to basement depths shown in figure 7. The inversion was restricted in each case by (a) 1 well, (b) 3 wells, (c) 6 wells, (d) 9 wells, (and) 12 wells, (f) 15 wells.

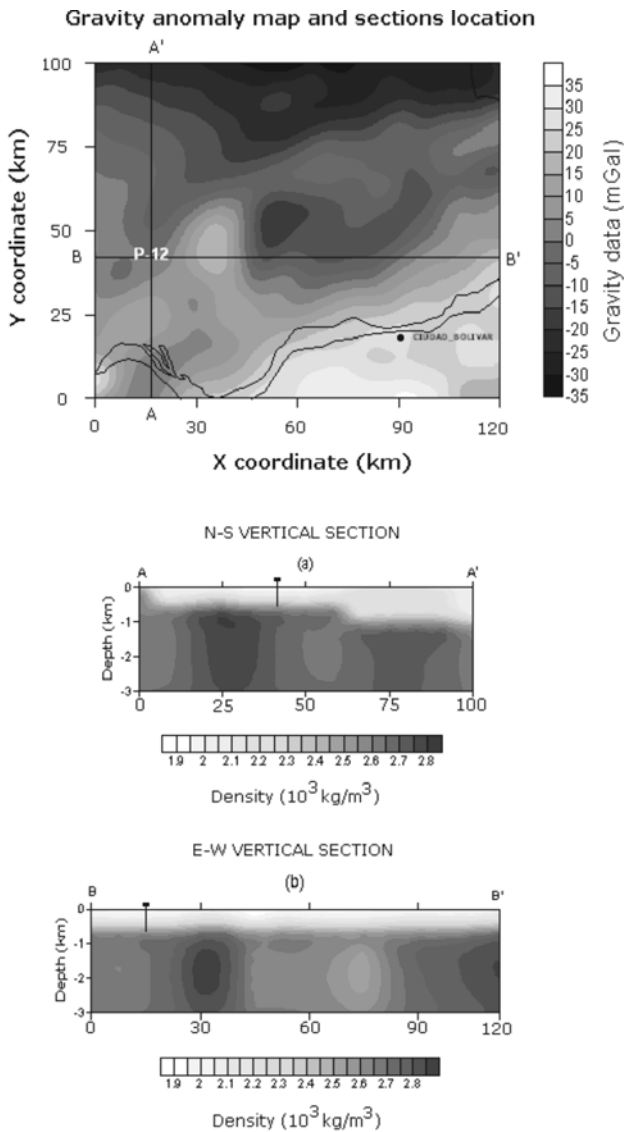


Figure 9. Location of the trace of two vertical sections intercepting the well P-12, superposed to the observed gravity field, and corresponding vertical section of the mass density estimated by the inversion for the case of 15 well constraints (a) in direction N-S and (b) in direction E-W.

reported in the well-logs of the blind group (group B) and calculate the corresponding rms prediction error for the depth of the basement. Also, we calculate the basement depth rms prediction error corresponding to the prior mean basement (shown in Figure 6). We recall that the latter is an estimation based only in the geostatistical interpolation of well data with no use of the gravity information. Figure 12 shows the plots of the rms basement depth prediction errors for the geostatistical inversion of gravity data and the plain geostatistical interpolation of well data. Additionally, the inversion of gravity data without well constraints produced an rms basement depth prediction error of 270 m that is also indicated in Figure 12. Results show that in the range

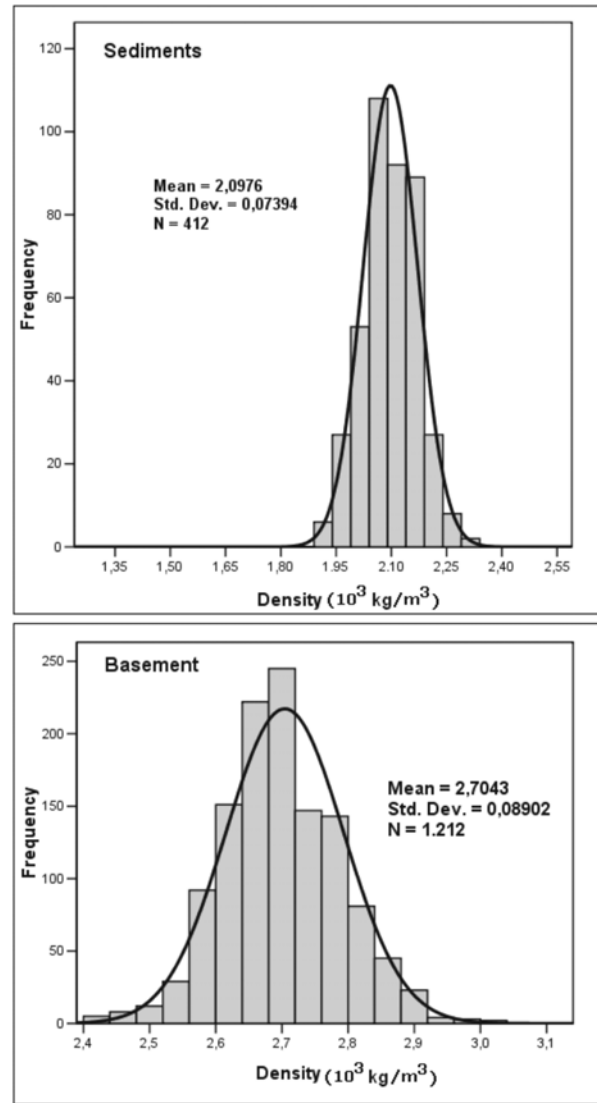


Figure 10. Histograms of mass density of sediments and basement, obtained from the estimated mass density model in the geostatistical inversion of gravimetric data for the 15 well constraints case.

between 1 and 6 wells, the geostatistical inversion of gravity data with well constraints performs better in predicting the depth of the basement than the gravity inversion with no well control or the Kriged basement estimated from the well data alone. For 6 or more wells the basement prediction based on the combination of gravity and well information produced equivalent results than the prediction based on the well information alone.

DISCUSSION

Results on the accuracy of the prediction indicate that the inversion of gravity data with depth controlled by well data

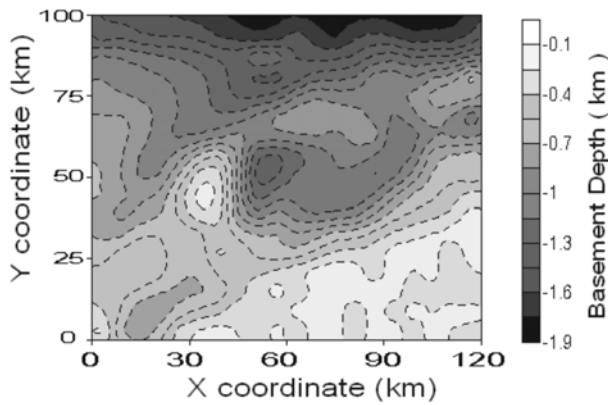


Figure 11. Basement depths estimated from the geostatistical inversion of gravity data with no well constraints on the basement interface.

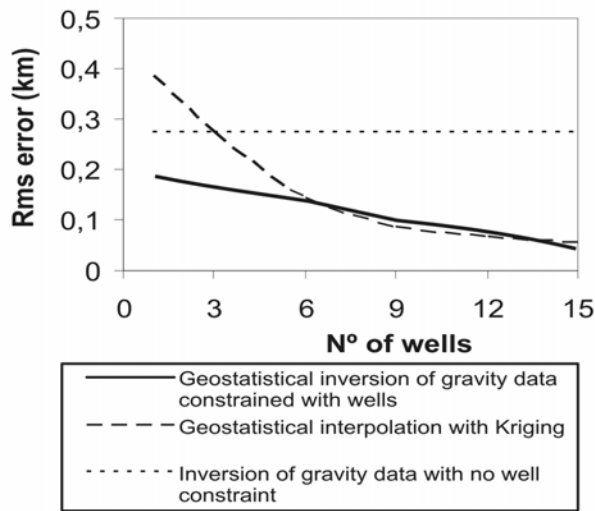


Figure 12. Root mean of squares (rms) prediction error for the basement depth in the wells not used in the inversion. The dashed line corresponds to estimates based only on well information (Kriging). The solid line corresponds to results of the inversion that combines gravimetric information and wells (geostatistical inversion of gravity data). The dotted horizontal line indicates the rms prediction error for the geostatistical inversion with no well constraint.

(at least at one point) improved the basement depth prediction significantly compared with the inversion of gravity data with any depth constraint. This can be considered an expected result. Several authors have shown (Pilkington & Crossley, 1986) that the potential field data have more information on relative depths of basement features than on their absolute depths, due to the joint data dependency on interface depth and property contrast. Hence, having one or more controlled depth points on the

basement interface should significantly improve the depth prediction.

On the other hand, in the range between 1 and 6 wells constraining the basement, the combination of gravity and well data, via the geostatistical gravity inversion, performed better than the interpolation of well data alone. This can also be considered an expected result as the gravity data contains information on the basement geometry. Well logs have accurate information on the depth of the basement, but the spatial distribution of wells could be scarce to sample basement features satisfactorily. Hence, the estimation of basement depths between the wells should be improved by the gravity data. As an example, for the first case (a single well in the group A) the estimation of basement depths in the blind wells (group B) based on the combination of the gravimetric information and the basement depth constraint on that well, reduces the prediction error in a half in comparison with the estimation based on well information alone. We can see, comparing Figure 7a and Figure 3, that in this case the inversion predicts the NS gradient of the basement depths, information that is impossible to obtain from a single well. For the determination of this tendency the gravimetric data were fundamental. Again, for the second case (3 wells in the group A) the prediction error of the combined estimate (gravity + wells) is approximately 2/3 of the prediction based only on well information. Also due to the gravimetric information the basement model predicted by the gravimetric inversion (Figure 7b) represents better the basement geometry than their equivalent *a priori* one based on the three well constraints alone.

More insight in the information content of the gravity data is needed to understand why above certain number of wells, the prediction based in gravity and well data are equivalent to the prediction based on well data alone. We explain this result throughout the fact that the gravimetric anomaly contains information of different sources, and not only on the basement depth. Therefore, the effects of the mass density variations, above and beneath the surface between sediments and basement, will produce deviations in the inversion estimate of the basement from their true value. This effect should be dependent on the area characteristics and well control. As a clear example, the couple of minimum and maximum of the gravity anomaly that can be seen in the center of the area do not represent in this area a structure related with the depth of the basement, but instead it is related with the changes of density in the crystalline basement (see gravity data and density sections in Figure 9). Significant changes of density and composition of the crystalline basement are also observed in other parts of the area, like in the Guayana Shield (González *et al.* 1980) where the crystalline basement is exposed. On the other hand, the

regional gradient of the gravity anomaly is well related with the basement geometry in the area, and this information improves the basement prediction when well information is poor in its spatial distribution.

CONCLUSIONS

In this work we describe a method to combine the gravimetric information with well-log information for the estimation of the major geologic layer geometry and density fields in 3-dimensions. The resulting model jointly explains the gravity observations, satisfies the conditions on the statistical distribution of the mass density and honors well-known positions of the layer interface. We applied this method to a region in eastern Venezuela and described the effect of gradually increasing the number of wells taken into account in the inversion on the basement depth prediction.

Our results indicate that the combination of gravity and well-log information for basement determination always improves basement prediction when compared with a gravity inversion with no well control. On the other hand, it also improves the basement prediction compared with an estimation purely based on well control when the spatial distribution of wells is scarce. When the spatial distribution of wells is dense enough both methods provide equivalent results in basement depth prediction. Additionally, the geostatistical gravity inversion provides information on the structure inside the layers related with the spatial variations of the density field.

ACKNOWLEDGEMENTS

We want to acknowledge the following institutions for partial support to this research: the CDCH of the Universidad Central de Venezuela (PG-0800-5631-2008), Geodinos-Fonacit (F-200200478), Conicit (199801098) and PDVSA-Intevep. Authors wish to thank PDVSA and Ameriven for providing the well and gravity data used in this work. We thank Freddy Fernandez (Intevep-PDVSA) for his cooperation with this research.

REFERENCES

- BARBOSA, V., SILVA, J., MEDEIROS, W. (1997a). *Gravity inversion of basement relief using approximate equality constraints on depths*: Geophysics, 62, 1745-1757.
- BARBOSA, V., SILVA, J., MEDEIROS, W. (1999b). *Gravity inversion of a discontinuous relief stabilized by weighted smoothness constraints on depth*: Geophysics, 64, 1429-1437.
- BEAR, G. W., AL-SHUKRI, H. J., RUDMAN, A.J. (1995). *Linear inversion of gravity data for 3-D density distributions*: Geophysics, 60, 1354-1364.
- BHASKARA, R. D. & RAMESH, B. N. (1991). *A fortran-77 computer program for three-dimensional analysis of gravity anomalies with variable density contrast*: Computers & Geosciences, 17, 655-667.
- BOSCH, M. (1999). *Lithologic Tomography, from plural geophysical data to lithology estimation*: Journal Geophysical Research, 174, 749-766.
- BOSCH, M. & MCGAUGHEY, J. (2001). *Joint inversion of gravity and magnetic data under lithologic constraints*: The Leading Edge, 20, 877-881.
- BOSCH, M., GUILLÉN, A., LEDRU, P. (2001). *Lithologic Tomography: An application to geophysical data from the Cadomian belt of northern Brittany, France*: Tectonophysics, 331, 197-227.
- BOSCH, M., MEZA, R., JIMÉNEZ, R., HÖNIG, A. (2006). *Joint gravity and magnetic inversion in 3D using Monte Carlo methods*, Geophysics, 71, G153-G156.
- FEO-CODECIDO, G., SMITH, F. JR., ABOUD, N., DI GIACOMO, E. (1984). *Basement and Paleozoic rocks of the Venezuelan Llanos Basins*: Geological Society of America, Memoir 162, 173-187.
- GONZÁLES, C., ITURRALDE DE AROZENA, J., PICARD, X. (1980). *Geología de Venezuela y sus cuencas petrolíferas*, Ed. Fonives, Caracas.
- GRATEROL, V. & GUMERT, W. (1998). *3-D gravity inversion with variable datum*: The Leading Edge, 17, 1769-1772.
- ISAAKS, E.D. & SRIVASTAVA, R.M. (1989). *Applied Geostatistics*: Oxford Univ. Press.
- JIMÉNEZ, R., BOSCH, M., FERNANDEZ, F. (2002). *Inversión Geoestadística de Datos Gravimétricos en la Región de Hamaca*, XI Congreso Venezolano de Geofísica.
- JIMÉNEZ, R., BOSCH, M. (2004). *Combinación de información gravimétrica y de pozos para la predicción del basamento en cuencas sedimentarias*, XII Congreso Venezolano de Geofísica.
- JIMÉNEZ, R. (2004). *Inversión Geoestadística 3D de Datos Gravimétricos: Aplicación a la Región Hamaca, Faja*

Petrolífera del Orinoco: M.Sc. thesis, Universidad Central de Venezuela.

LI, Y. & OLDENBURG, D. (1998). *3-D inversion of gravity data*: Geophysics, 63, 109-119.

MOSEGAARD, K. & TARANTOLA, A. (200). *Probabilistic Approach to Inverse Problems*, Chapter for the International Handbook of Earthquake and Engineering Seismology, IASPEI.

PILKINGTON, M. & CROSSLEY, D. J. (1986). *Determination of crustal interface topography from potential fields*: Geophysics, 51, 1277-1284.

RAMA, P., SWAMY, K. V., RADHAKRISHNA, I. V. (1999). *Inversion of gravity anomalies of three-dimensional density interfaces*: Computers & Geosciences, 25, 887-896.

RUSSO, R. M. & SPEED, R. C. (1994). *Spectral analysis of gravity anomalies and the architecture of tectonic wedging*, NE Venezuela and Trinidad: Tectonics, 13, 613-622.

TARANTOLA, A. (1987). *Inverse Problem Theory: Methods for Data Fitting and Model Parameter Estimation*: Elsevier, New York.